

P1.4 TETHERED-BALLOONE BORNE MEASUREMENTS OF THE FINE-SCALE STRUCTURE OF BOUNDARY LAYER CLOUDS

Holger Siebert and Manfred Wendisch

Institute for Tropospheric Research, Leipzig, Germany

1 INTRODUCTION

Boundary layer clouds play an important role for the weather forecast but also for climate research due to their significant impact on radiative transfer and, therefore, for the atmospheric energy budget. However, high resolution measurements of dynamical, thermodynamical, and microphysical properties in the cloudy boundary layer are still rare.

To overcome this lack of data an Airship-borne Cloud Turbulence Observation System, called ACTOS has been developed. Here, ACTOS is introduced and first data from measurements carried out during the BBC (Baltex Bridge Cloud) campaign performed in Cabauw, The Netherlands, in 2001 are presented.

2 EXPERIMENTAL SETUP

ACTOS is equipped with sensors to measure thermodynamical, dynamical, and microphysical (cloud droplet and particle) properties under cloudless and more challenging cloudy conditions. An ultrasonic anemometer/thermometer (sonic) is used to measure the three-dimensional wind vector and the virtual temperatur; for calibration a PT-100 thermometer is integrated. A navigation unit provides the lateral velocity, the attitude angles, and position of the sonic with respect to an Earth-fixed coordinate frame. The water vapour density ρ_v is measured with a Lyman- α hygrometer, a special pre-impactor inlet prevents from cloud drop penetration into the system. A capacitive sensor completes the humidity measurements.

Corresponding author's address: Holger Siebert,
Institute for Tropospheric Research,
Permoser Straße 15, 04318 Leipzig, Germany.
Email: siebert@tropos.de

The liquid water content (LWC) is measured with a particle volume monitor (PVM-100A). A condensation particle counter (CPC) measures aerosol particle number concentration (N_P) in the size range between 10 and 1000 nm.

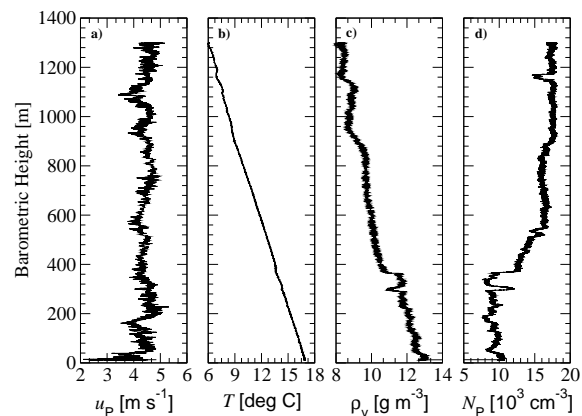


Figure 1: Vertical profiles of u_P , T , ρ_v , and N_P under cloud-free conditions.

While all parameters are available with 100 Hz temporal resolution, the N_P is available with about 1 Hz only. A complete system discussion can be found in Siebert (2001) and Siebert et al. (2001).

All sensors are integrated on an aerodynamic platform which is fixed 25 m below the balloon. The length of the platform is about 4 m, the weight is 100 kg, respectively. Two tail units keep the system in the mean wind direction and minimize the influence of flow distortions on the turbulence sensors.

For this experiment, the tethered balloon system “MAPS-Y” operated by the German Army was used. The hydrogen filled balloon is 24 m long and has a maximum diameter of 6.5 m. The ceiling of this system is about 1400 m at maximum wind speeds of 15 m s^{-1} .

3 DATA ANALYSIS AND RESULTS

During the BBC campaign several flights with AC-TOS were carried out. Here, data from the 12th of September 2001 are presented. Figure 1 shows vertical profiles of u_p , T , ρ_v , and N_P . The mean value of u_p was at about 4 to 5 m s^{-1} . T decreases nearly linear over the complete ascent from 16.5 to 6°C, that is, the temperature gradient γ was 0.8 K (100 m) $^{-1}$ which is slight subadiabatic. The ρ_v -profile shows a decrease with height with a significant local minimum in 300 m and a jump from 11.6 to 10.6 g m^{-3} in 360 m. This jump marks the boundary layer (BL) height. Above this height, ρ_v decreases again nearly linear with a few height constant layers above 600 m. While the corresponding temperature jump at the inversion in 360 m was only about 50 mK, which is close to the resolution of the sensors, N_P shows a very similar but opposite behaviour like ρ_v . The small inversion separates two complete different air masses. Within the BL the air has more water vapour and less particles, above the BL, the air mass is drier with more particles, respectively.

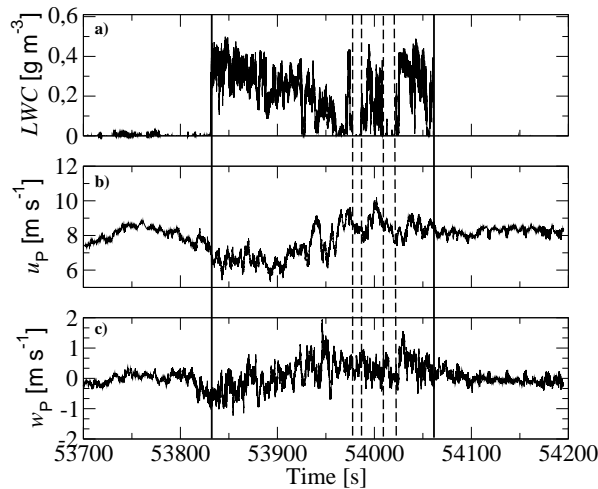


Figure 2: Time series of LWC , u_p , and w_p during a cloud penetration.

At the maximum height of the ascent the platform was fixed at a constant level. Several penetrations of small cumulus clouds were observed during this period. Figure 2 and 3 show time series of parameters measured during a cloud penetration between $t = 53835$ and 54065 s as marked with vertical solid lines. Figure 2a shows the LWC . Maximum values of about 0.45 g m^{-3} were observed.

In the second part of the cloud, the LWC shows much more scatter. This part includes also small drop-free parts marked with vertical dashed lines. Figure 2b and 2c show the longitudinal and vertical wind components u_p, w_p measured relative to the platform. The mean value of u_p was increased to about 8 m s^{-1} , both components show much more fluctuations within the cloud than outside.

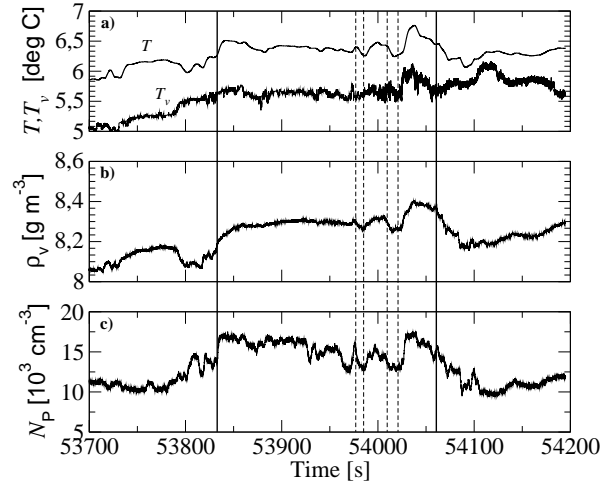


Figure 3: Time series of T , T_v , ρ_v , and N_P . The cloud region (cf. Fig. 2) is marked by vertical solid lines.

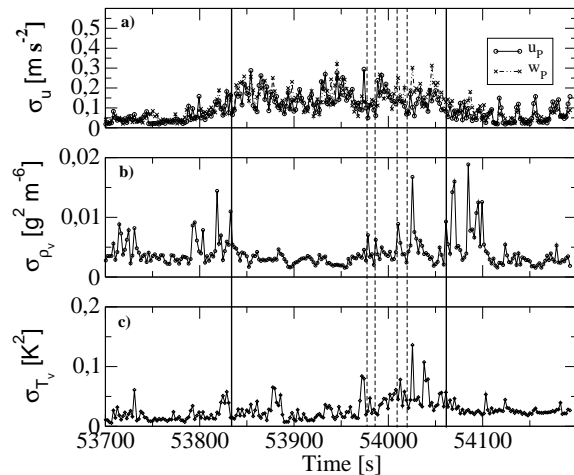


Figure 4: Time series of standard deviations σ_u , σ_{ρ_v} , and σ_{T_v} . Each point represents the standard deviation over 2 s (200 samples).

The standard deviations σ_u of the wind components are shown in Fig. 4a. The influence of the

cloud is obvious. The standard deviations during the cloud penetration are about 5 to 10 times higher than outside the cloud. Figure 3a shows the temperature time series measured with a PT-100 and the virtual temperature T_v measured with the sonic. However, the temperature signal shows more fluctuations at cloud edges (solid and dashed lines) than within the cloud part with LWC well above zero. The cloud influences on the fluctuations is not as obvious as for the wind fluctuations.

Figure 3b shows the time series of ρ_v which is slightly increased within the cloud. The cloud-free parts (dashed lines) can be identified as local minima in ρ_v . The fluctuations of ρ_v are much stronger outside the cloud or at cloud edges. The fluctuations are minimal in the first part of the cloud where the LWC is always well above zero (cf. Fig. 2a). N_P is increased within the cloud, while again the drop-free parts correspond with local minima in N_P . This behaviour can be explained only with advection of the cloudy air mass with general higher N_P .

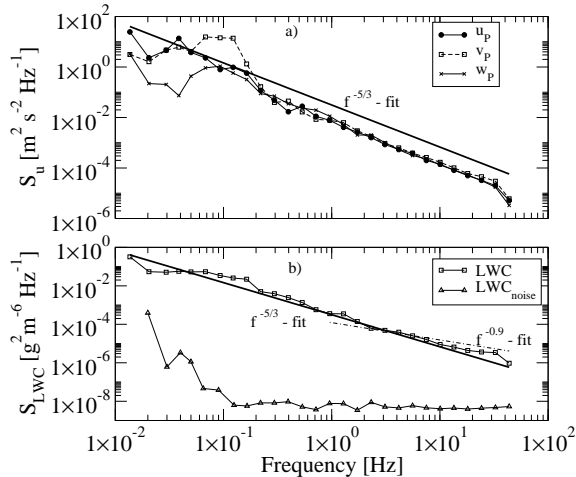


Figure 5: Power spectra of wind components S_u , liquid water content S_{LWC} measured inside the cloud.

Finally, one-sided frequency power spectra of u_P , v_P , w_P , LWC , ρ_v , and T_v are presented in Fig. 5 and 6. The raw spectra are calculated with a Fast Fourier Transformation (FFT) over a time period of 170 s. All data were measured inside the cloud. The noise spectrum of the PVM was calculated from a 100 s period after the cloud penetration. The raw spectra are averaged over logarithmic equidistant bins. A $f^{-5/3}$ -fit is included as

expected for an inertial subrange.

All three wind components show a clear inertial subrange behaviour between 0.2 and 30 Hz (cf. Fig. 5a). For higher frequencies the spectra drop off due to the anti-aliasing filter which was set for all shown quantities at $f_c = 30$ Hz. The lateral wind component v_p shows a significant peak around 0.1 Hz due to the pendulum of the platform. The LWC also shows a $f^{-5/3}$ behaviour but begins to flatten for frequencies higher than 20 Hz which corresponds with a mean wind speed of 8 m s^{-1} to a length scale of about 0.4 m. The noise level of the PVM can be estimated to $S_{LWC}^{(n)} \approx 5 \times 10^{-9} \text{ g}^2 \text{ m}^{-6} \text{ Hz}^{-1}$. With

$$\sigma^{(n)} = \sqrt{S_{LWC}^{(n)} \times f_{Ny}} \quad (1)$$

a standard deviation due to uncorrelated noise of $\sigma^{(n)} \approx 5 \times 10^{-4} \text{ g m}^{-3}$ is found. This is much below the observed value close to the Nyquist frequency of the spectrum measured inside the cloud.

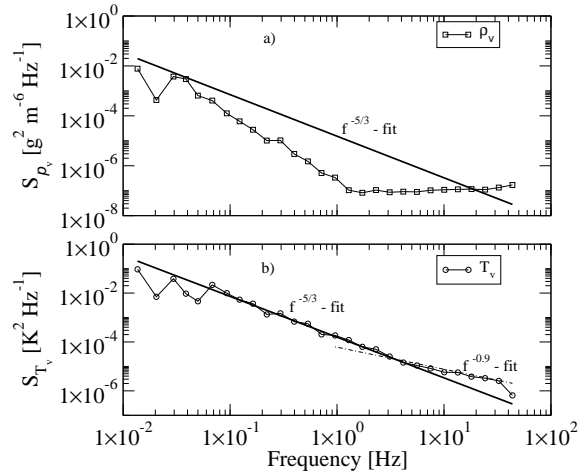


Figure 6: Power spectra of water vapour density S_{ρ_v} and virtual temperature S_{T_v} measured inside the cloud.

A similar behaviour is observed in the spectrum of T_v (cf. Fig. 6b) which also shows an inertial subrange behaviour up to about 4 Hz and then begins to flatten. The spectrum of the water vapour density S_{ρ_v} (cf. Fig. 6a) shows a drop-off steeper than $-5/3$ due to averaging effects in the pre-impactor inlet and tubes. At a frequency of 2 Hz the signal becomes noisy. The noise level is estimated to about $10^{-7} \text{ g}^2 \text{ m}^{-2} \text{ Hz}^{-1}$ which leads to a standard deviation due to noise of $\sigma_{\rho_v}^{(n)} = 2 \times 10^{-3} \text{ g m}^{-1}$.

There are several possible explanations for the flatten of the power spectra as observed for the LWC and T_v . First, flow distortions around the platform may lead to higher variances than expected for an inertial subrange. For the PVM data this explanation is possible because the typical dimensions of the front part of the platform are in the order of half a meter. The PVM could not be placed as far away from the platform like the sonic or other turbulence sensors due to mechanical constraints. T_v is measured with the same sensor as the wind speed which spectra show no flatten. That means, it is unlikely that flow distortions around the sonic should be responsible for this effect. So-called “scale-breaks” in power spectra due to mixing effects as mentioned by Davis et al. (1999) or Malinowski et al. (2000) also lead to an increased variance at length scales in the order of several meters. The slope observed in the spectrum of T_v for higher frequencies is close to -0.9 as observed by Davis et al. (1999) for LWC spectra. However, no final explanation for the behaviour observed in our data can be presented here.

4 ACKNOWLEDGEMENTS

We thank T. Conrath and D. Schell for their excellent technical support during the BBC campaign.

The balloon was operated by G. Sanftleben and his crew from the German Army (WTD-71, Eckernförde).

5 REFERENCES

- Davis, A. B., A. Marshak, H. Gerber, and W. J. Wiscombe: 1999, ‘Horizontal structure of marine boundary layer clouds from centimeter to kilometer scales.’. *J. Geophys. Res.* **104**, 6123–6144.
- Malinowski, S., K. E. Haman, M. Andrejczuk, P. Banat, and A. Jaczewski: 2000, ‘Small-scale properties of clouds: Summary of recent results from aircraft measurements, laboratory experiments and numerical modeling.’. In: *Preprints 13th International Conference on Clouds and Precipitation*. Reno/Nevada (14-18 August 2000).
- Siebert, H.: 2001, ‘Tethered-balloon borne turbulence measurements in the cloudy boundary layer’. Ph.D. thesis, University of Leipzig, Germany, 122 p.
- Siebert, H., M. Wendisch, T. Conrath, U. Teichmann, and J. Heintzenberg: 2001, ‘A new tethered balloon-borne turbulence platform for fine-scale observations within the cloudy boundary layer’. *Boundary-Layer Meteorol.* submitted.